

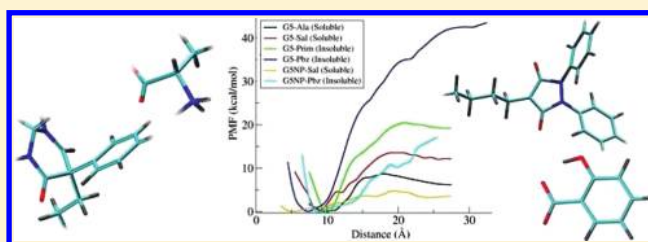
PAMAM Dendrimer–Drug Interactions: Effect of pH on the Binding and Release Pattern

Vishal Maingi, Mattaparthi Venkata Satish Kumar, and Prabal K. Maiti*

Centre for Condensed Matter Theory, Department of Physics, Indian Institute of Science, Bangalore 560 012, India

S Supporting Information

ABSTRACT: Understanding the dendrimer–drug interaction is of great importance to design and optimize the dendrimer-based drug delivery system. Using atomistic molecular dynamics (MD) simulations, we have analyzed the release pattern of four ligands (two soluble drugs, namely, salicylic acid (Sal), L-alanine (Ala), and two insoluble drugs, namely, phenylbutazone (Pbz) and primidone (Prim)), which were initially encapsulated inside the ethylenediamine (EDA) cored polyamidoamine (PAMAM) dendrimer using the docking method. We have computed the potential of mean force (PMF) variation with generation 5 (G5)-PAMAM dendrimer complexed with drug molecules using umbrella sampling. From our calculated PMF values, we observe that soluble drugs (Sal and Ala) have lower energy barriers than insoluble drugs (Pbz and Prim). The order of ease of release pattern for these drugs from G5 protonated PAMAM dendrimer was found to be Ala > Sal > Prim > Pbz. In the case of insoluble drugs (Prim and Pbz), because of larger size, we observe much nonpolar contribution, and thus, their larger energy barriers can be reasoned to van der Waals contribution. From the hydrogen bonding analysis of the four PAMAM–drug complexes under study, we found intermolecular hydrogen bonding to show less significant contribution to the free energy barrier. Another interesting feature appears while calculating the PMF profile of G5NP (nonprotonated)-PAMAM–Pbz and G5NP (nonprotonated)-PAMAM–Sal complex. The PMF was found to be less when the drug is bound to nonprotonated dendrimer compared to the protonated dendrimer. Our results suggest that encapsulation of the drug molecule into the host PAMAM dendrimer should be carried out at higher pH values (near pH 10). When such complex enters the human body, the pH is around 7.4 and at that physiological pH, the dendrimer holds the drug tightly. Hence the release of drug can occur at a controlled rate into the bloodstream. Thus, our findings provide a microscopic picture of the encapsulation and controlled release of drugs in the case of dendrimer-based host–guest systems.



1. INTRODUCTION

In the recent past, we see the rapid rise in application of nanotechnology in the field of biomedicine that includes drug and gene delivery,¹ diagnostic techniques,² and tissue engineering.³ Nowadays, a number of nanomaterials such as lipid-, polymer-, and metal-based nanoparticles has been frequently used as nanovehicles for drug delivery applications. This is mainly because the nanomaterials do the effective delivery of conventional drugs to the target subcellular region without the necessity of change in the structure of the drugs.⁴ The versatile properties of dendrimers, such as hyperbranched structure, well-defined molecular weight, size, and globular shape, monodisperse nature, as well as having a high functional surface makes them to be considered as a promising candidate for a wide range of biological applications (drug delivery, siRNA delivery, cancer diagnostics, solubility improvement, imaging),^{5–12} catalysis,^{13–16} electronics,¹⁷ and many more. There is tremendous increase in the importance of dendrimer based drug delivery systems in the pharmaceutical sciences.^{18–24} For the improved drug delivery by means of host–guest system of dendrimer–drug complexes, we have to understand clearly the interactions between the dendrimer and the drug. The

interactions between drug and the dendrimer have been studied^{25,26} in recent years and are broadly divided into two categories: entrapment of drugs within the dendrimer architecture (this generally involves electrostatic, hydrophobic and hydrogen bond interactions) and the other one is interaction between drug and the surface of the dendrimer (this includes electrostatic interactions and covalent bonding). The surface interactions between the drug and the dendrimer have been found to be dependent on the availability of the potential surface groups on the dendrimer surface. These types of interactions between the drug and the dendrimer have been used to study the controlled release of drug and thereby to boost the drug efficiency.

In most of the recent studies, the encapsulation of drug within the dendrimer core structure occurs by a simple physical entrapment involving nonbonding interactions, and also, the binding mode of the drug to the dendrimer was found to depend not only on size, pK_a , nature of functional groups, and

Received: November 30, 2011

Revised: February 27, 2012

Published: March 14, 2012

structure of drug but also on the dendrimer generation, core structure, and surface charge of dendrimers.^{8,9,27,28}

PAMAM dendrimer, which has large number of cationic surface groups and internal amine groups, offers both surface binding as well as encapsulation of the guest such as drug molecules. This type of binding involves hydrophobic and external electrostatic as well as hydrogen bonding interactions.^{9,28,29} It was also found that dendrimers of higher generation are better capable of encapsulating guests in the interior compared to a lower generation dendrimer. For lower generation dendrimers, surface binding is easier due to electrostatic interaction on surface.²⁸ For guest with low pK_a values, the internal electrostatic interactions also play an important role.³⁰

Astruc et al.³¹ suggested a host–guest interaction model in which the first step is the ionic interaction between an oppositely charged dendrimer and a guest molecule followed by hydrophobic encapsulation. It was further suggested by Jingjing et al.³⁰ that, even for release behavior of host–guest, electrostatic interactions play an important role, as it was observed in case of the mycophenolic acid–dendrimer complex while changing pH conditions. Several works have demonstrated that, for a dendrimer–ligand complex, the electrostatic force, hydrophobic interaction, hydrogen-bond interaction, and van der Waals force influence not only complex formation but also the release pattern of guests.^{32,33}

Recent study by Zhao et al.³⁴ on high-throughput screening of dendrimer-binding drugs by NMR techniques motivated us to study the drug–dendrimer complexes at the atomistic level. They found competitive binding between the ligands in the screening pool and the dendrimer. Their work has pointed out the salient features for the physicochemical properties of dendrimer based host–guest systems and design of dendrimer-based drug formulations.

One of the early MD studies for such dendrimer complexes was carried out by Goddard and co-workers on the terminally modified fifth generation poly(propyleneimine) dendrimer encapsulating Bengal–Rose molecules.³⁵ A close agreement with the experimental findings was seen in such study in which a number of ligand molecules were entrapped in the interior of the dendrimer. Later, MD simulation was used to study the interaction of eosin dye with dansyl terminated fourth generation propylene amine dendrimer. This study shows the flexibility of dendrimer and mobility of guest molecules inside dendrimer.³⁶ An MD approach was used to refine the molecular model proposed for PAMAM–agonist (CGS21680) bound to the A_{2A} adenosine receptor dimer.³⁷ Efficient encapsulation was noticed in the interior of the backfolded molecule compared to the extended isomer.³⁸ Apart from these studies, there are very few theoretical MD studies.^{39–44}

In the present work, we have examined the release pattern behavior for each of the four ligands (Sal, Ala, Prim, and Pbz), which were encapsulated initially inside the protonated dendrimer (corresponding to the neutral pH case). In addition to these, we have also examined the release pattern behavior of two drugs, Sal and Pbz, from the nonprotonated dendrimer (corresponding to high pH case). To understand the free energy difference between the free and bound states of ligands with dendrimer, we have computed the PMF variation between the G5-PAMAM dendrimer and the four ligand/drug molecules by using umbrella samplings with distance-based biasing potential without directional restraints.⁴⁵ From the PMF difference between the bound (ligand–dendrimer complex) and free

forms, we have studied the ease in release of ligands from the interior of the dendrimer.

2. COMPUTATIONAL METHOD

To mimic the experimental conditions, we have used protonated and nonprotonated G5-PAMAM dendrimer as the host molecule for several drug candidates selected from the work of Zhao et al.³⁴ The starting coordinates and restrained electrostatic potential (RESP) charges for G5-PAMAM were taken from our previous works.⁴⁶ Four drug molecules, two soluble (Ala and Sal) and two insoluble (Prim and Pbz), were chosen for this study. Figure 1 shows the molecular structure of four drug molecules used in this study. All the structures were optimized using Gaussian03 with HF/6-31G(d) as the basis set. Gaussian output files of the optimized drug molecules were used to calculate RESP charges using AMBER.^{47,48} In this study, we have performed simulation at neutral pH ($pH \approx 7$) and high pH ($pH \approx 10$). In neutral pH medium, Pbz, which has $pK_a \approx 4.5$, and Sal, which has $pK_a \approx 3$, exist mainly in anionic form. Prim with $pK_a \approx 12$ exists mainly in neutral form. In contrast, Ala (an amino acid) exists as a zwitterion at neutral pH. At high pH ($pH \approx 10$), Pbz and Sal exist in anionic form because of their low pK_a values. So, in our simulation, we have considered anionic Pbz and Sal, neutral Prim, and zwitterionic Ala.

General Amber Force Field (GAFF) was used to describe the inter- and intramolecular interactions.⁴⁹ In Table S1 of the Supporting Information, RESP charges for all of the drug molecules studied in this work are provided.

2.1. Docking. We obtained the starting coordinates for the G5-PAMAM–drug complexes using a docking procedure as outlined below. The four drug/ligand molecules were docked separately in the interior of G5-PAMAM dendrimer using AutoDock Vina.⁵⁰ For the visual help, center of grid points, and box selection, AutoDock4 was used.⁵¹ The center of grid box was chosen in such a way that search space for a drug molecule limits to the central region of G5-PAMAM dendrimer, closer to the ethylene diamine core. The number of grid points along the x , y , and z directions were chosen to be 20. Thus, the central part, which included the core of dendrimer along with additional residues of G5-PAMAM, was covered by the grid box. The grid spacing was set to 1 Å. This process can be considered as blind docking. During docking, the charges were kept the same as those that were obtained from RESP calculations for both dendrimer and drug molecule.⁴⁶ The nonpolar hydrogens were not allowed to merge. In the case of Sal, if the bond rotations are allowed during docking, the intramolecular hydrogen bonding conformation is not obtained. So during the docking process, the two bond rotations were not allowed, but for MD simulations, no such restriction was imposed. The best scoring docked conformation was selected in each case. For the neutral pH case, the coordinates of the G5-PAMAM–Phenylbutazone (G5–Pbz), G5–primidone (G5–Prim), G5–salicylic acid (G5–Sal), and G5–alanine (G5–Ala) complexes were obtained from AutoDock4. In the similar manner, the starting coordinates for G5NP-PAMAM–phenylbutazone (G5NP–Pbz) and G5NP-PAMAM–salicylic acid (G5NP–Sal) were obtained.

2.2. Molecular Dynamics Simulation. All MD simulations were performed using the AMBER9 package with GAFF set of parameters. The G5–Pbz, G5–Prim, G5–Sal, and G5–Ala complex obtained using docking as outlined in the previous section were solvated using TIP3P water,⁵² with solvent buffer

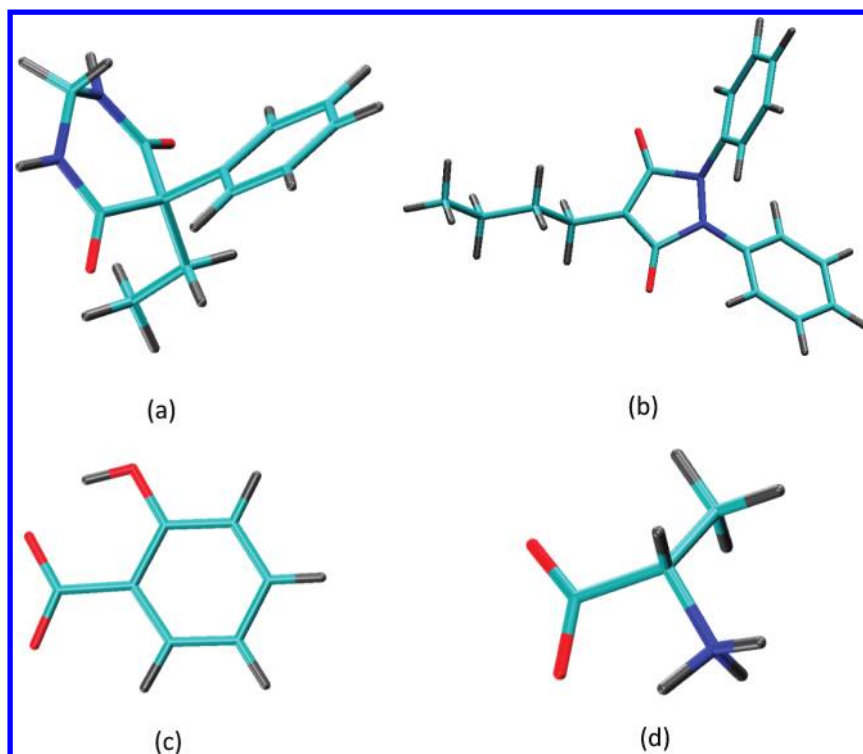


Figure 1. Four ligands used for complex formation with G5-PAMAM: (a) primidone, (b) phenylbutazone, (c) salicylic acid, and (d) L-alanine. Color codes: cyan, carbon; blue, nitrogen; red, oxygen; and gray, hydrogen.

being 10 Å in all directions. In addition, some waters were replaced by Na^+ counterions to neutralize the negative charges on the Pbz and Sal. Then, appropriate numbers of Cl^- ions were added to neutralize the positive charges on the dendrimer amine sites for the protonated G5-PAMAM. Similar protocol was used to prepare the system for the G5-Ala and G5-Prim complexes also. In the case of nonprotonated G5, no Cl^- ions were added.

The solvated structures were then subjected to 1000 steps of steepest descent minimization of the potential energy, followed by 2000 steps of conjugate gradient minimization. During this minimization, the dendrimer–drug molecule was kept fixed in its starting conformation using harmonic constraint with a force constant of 500 kcal/mol/Å². This allowed the water molecules to reorganize to eliminate bad contacts with the dendrimer molecule. This was followed by another 5000 steps of conjugate gradient minimization while decreasing the force constant of the harmonic restraints from 20 kcal/mol/Å² to zero in steps of 5 kcal/mol/Å². The minimized structure was initially subjected to 40 ps of MD, using a 2 fs time step for integration. During the MD, the system was gradually heated from 0 to 300 K using weak 20 kcal/mol/Å² harmonic constraints on the solute to its starting structure. This allows for slow relaxation of the built dendrimer–drug structure. The NVT dynamics was done using the SHAKE⁵³ method with a geometrical tolerance of 5×10^{-4} Å being imposed on all covalent bonds involving hydrogen atoms. The electrostatics interactions were evaluated with the particle mesh Ewald (PME) method,⁵⁴ using a real space cut off of 9 Å.

For each complex, G5-Pbz, G5-Prim, G5-Sal, and G5-Ala, starting coordinates for the umbrellas sampling runs were taken from the restart file that has been obtained after running 1 ns NVT run dynamics. Umbrella samplings were performed with a reaction coordinate being the distance between the center of mass (COM) of all atoms of drug (Pbz, Prim, Sal, or Ala)

and COM of central five residues of dendrimer (core aaa and four bbb attached to aaa core; total 140 atoms. For the umbrella sampling, a harmonic potential with a spring constant of 2 kcal/mol/Å² was used. A detailed description of residues can be found in our earlier work⁴⁶). Figure 2 explains the method



Figure 2. Steps followed for collecting umbrella samples. S is starting point, I is representing toward the inside when COM (ligand)–COM (dendrimer) distance is decreased from S point, and O is representing toward the outside when COM (ligand)–COM (dendrimer) distance is increased from S point until ligand was released. In both cases, going from S to O and S to I, the restart file of the previous step was used. Please refer to Table 1 also.

for collecting histogram at various umbrella windows. Further windows were obtained by an increment of 1 Å. For each window, 1 ns NVT dynamics was performed, and the resulting equilibrated structure was used as the starting coordinate for the next window. Some windows were obtained by decreasing the COM (ligand)–COM (dendrimer) distance to obtain the PMF values at closer distance between the drug and dendrimer. For the four complex systems under study, we have calculated the PMF using the weighted histogram analysis method (WHAM).⁵⁵ Starting distance between COM ligand–COM PAMAM and total duration for umbrella sampling can be seen in Table 1.

3. RESULTS AND DISCUSSION

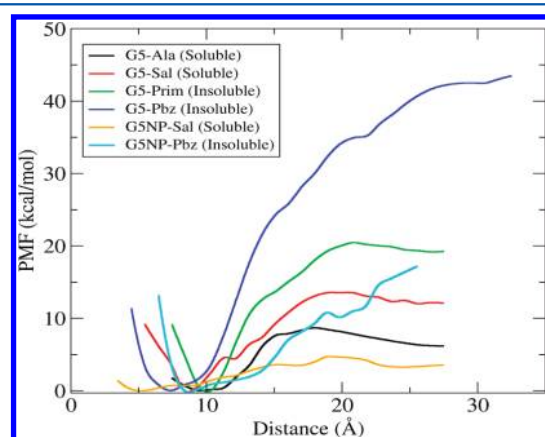
The potential of mean force (PMF) variation between free form and bound form of drug with the dendrimer as a function

Table 1. Comparison of Various Complexes with Respect to Their Starting Configurations in Terms of Distance Only

complex	starting distance between COM ligand–COM PAMAM (Å) ^a	distance sampled (Å)	duration (ns) for umbrella sampling; each window size being 1 ns
G5NP–Pbz	7.36	6 to 27	22
G5–Pbz	7.89	4 to 33	30
G5–Prim	10.41	7 to 28	22
G5NP–Sal	9.04	3 to 28	26
G5–Sal	7.71	5 to 28	24
G5–Ala	10.91	7 to 28	22

^aCenter of mass (COM) considering all atoms of ligand and COM PAMAM is for central five residues (core aaa and four bbb attached to aaa core).

of distance between the dendrimer core and drug is shown in Figure 3. From the figure, we observe that in the case of

**Figure 3.** PMF variation as a function of the drug–dendrimer center of mass distance for all the cases studied in this work.

protonated G5 dendrimer, soluble drugs (Sal and Ala) have a lower free energy barrier when compared to the insoluble drugs (Pbz and Prim). Among all the drugs studied, Ala shows the lowest free energy barrier and thus expected to get released from the interior of the dendrimer with ease. The free energy difference between Pbz with Prim, Sal, and Ala was found to be approximately 23, 29, and 35 kcal/mol, respectively. The equilibrium snapshot for each of the four cases at the minimum of PMF is shown in Figure 4.

From the PMF plot, we see the order of ease of release pattern of drugs from G5 protonated PAMAM dendrimer to be Ala > Sal > Prim > Pbz. This order of release pattern depends on factors such as solubility, size, and charge on the drug molecules. It is known that the electrostatic interaction is the driving force for the encapsulation of drug into the dendrimer core, but in the high-throughput screening of dendrimer-binding drugs, Zhao et al.³⁴ observed the dendrimer molecule to show low tendency to encapsulate the hydrophilic drug molecules (Sal and Ala) into its core region, although Sal and Ala drug molecules contain negative charges in their structure. However, they also observed strong encapsulation of some of the insoluble drugs that carries negative charges in their structures (Pbz) into the interior pockets of the dendrimer. Among the insoluble drug pool, they found Pbz as one of the ligands showing much interaction with dendrimer scaffold

protons. The other drug molecule (Prim), which is insoluble but neutral, shows lower tendency to encapsulate inside the dendrimer. This is due to the absence of electrostatic interaction as Prim is a neutral molecule. They also noticed that hydrophilic drug molecules (Sal and Ala) bearing some charges in their structures to be involved in competitive binding (due to ionic interactions) on the surface of dendrimer. In our PMF study, we observe a lower free energy barrier for the Sal and Ala drug molecules. This may lead us to think that a large amount of these drugs can be encapsulated and can also be released easily from the dendrimer core, but in the experimental study, Zhao et al.³⁴ found very little or no drug (Sal or Ala) encapsulated inside the core of the dendrimer. So, from the experimental results³⁴ and from our PMF analysis, we can conclude that, although Sal and Ala drug molecules have lower free energy barrier, it is difficult to encapsulate them inside the dendrimer. This is because of the absence of nonpolar groups in their chemical structure, thus making less van der Waals contribution. Since these drugs contain polar groups in their structure, they prefer to stay on the surface of the dendrimer where much water is available. However, we observe larger energy barriers for the insoluble drugs (Prim and Pbz) because of their stronger nonpolar contribution and larger sizes leading to high van der Waals contribution. Also, it is a well-known fact that van der Waals contribution increases as the nonpolar part increases. In our study, we assumed internal (tertiary) amines to be nonprotonated, so there is no contribution from internal electrostatic interaction. So the energy barrier can be correlated to hydrogen bond and van der Waals interactions, as the ligand is moved away from the core of the dendrimer. Because of the back folding in the interior of the dendrimer, terminal protonated primary amines can also contribute to external electrostatic interactions.

In Figure 5, we plot the number of intermolecular hydrogen bonds for each window for the umbrella sampling runs for all the four PAMAM–ligand complexes in the case of protonated dendrimer. For calculating the hydrogen bond, the cut off for angle and distance was set to 120° and 3.5 Å, respectively. Hydrogen bond analysis in all the four cases show no or lower number of hydrogen bonds when the distance between the ligand and PAMAM dendrimer is between 12 Å to 17 Å. In this distance range, the drug is in the hollow part of the dendrimer and may be in the cavity where hydrogen bond formation cannot happen. The number of intermolecular hydrogen bonds increases when the distance between the ligand and dendrimer is less than 12 Å, which corresponds to a near core region and again at around 25 Å. The higher distance corresponds to the radius of gyration (approximately 25 Å) of G5-PAMAM dendrimer, and hence, at this distance, there are a number of terminal protonated amine groups that help in hydrogen bonding, and also, electrostatic interactions can be expected at this region with charged ligands.

High free energy barrier is expected from the ligand showing larger number of intermolecular hydrogen bonds. Comparing the PMF profiles of Pbz and Ala, it can be observed (from Figures 3 and 5) that hydrogen bonding alone does not play much role in increasing the free energy barrier for release of ligands. For example, in the case of Ala, we find a relatively higher number of hydrogen bonds in each window, but it possesses the lowest free energy barrier.

Another very interesting feature appeared when we calculated the PMF profile of G5NP-PAMAM dendrimer complexed with Pbz. We found the energy barrier for G5NP-PAMAM–Pbz

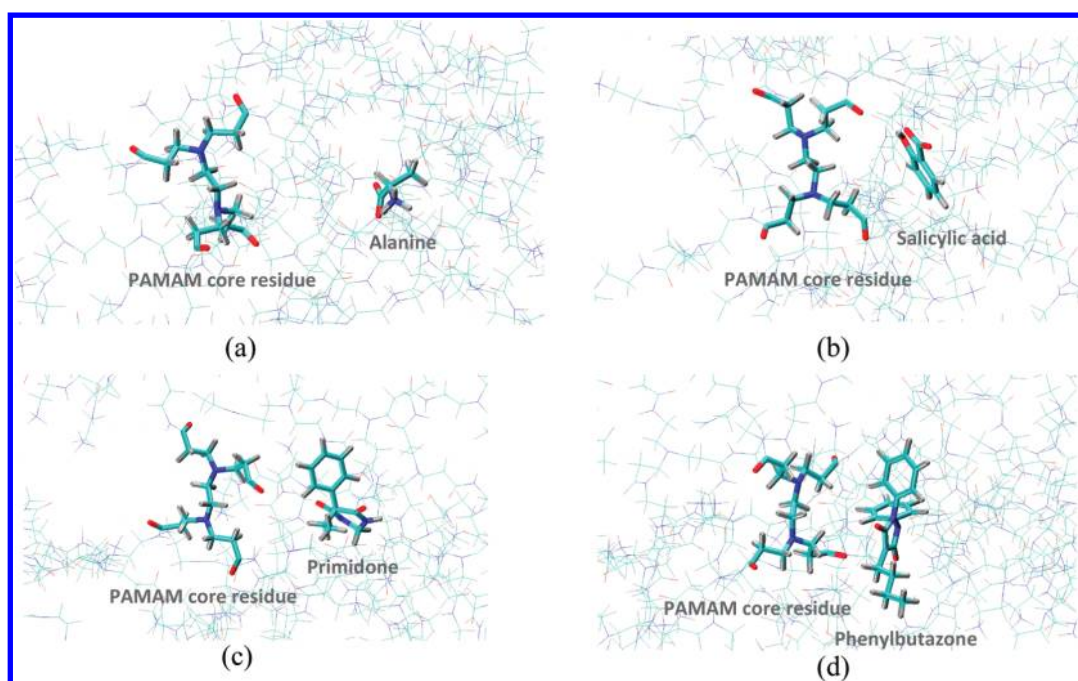


Figure 4. Equilibrium snapshot for each of the four cases at the minimum of PMF values. (a) G5-PAMAM–Ala complex, (b) G5-PAMAM–Sal complex, (c) G5-PAMAM–Prim complex, and (d) G5-PAMAM–Pbz complex. Central residue and ligands are shown as thick bonds and remaining part of dendrimer (not fully shown) as thin stick bonds.

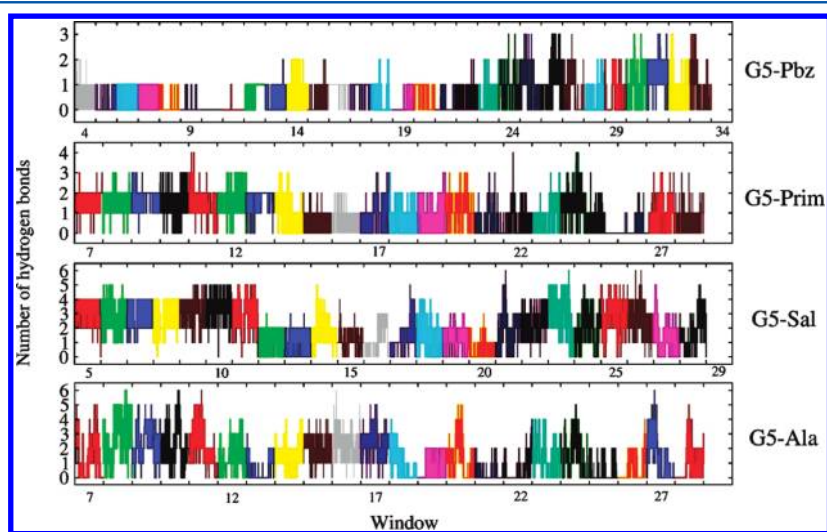


Figure 5. Intermolecular hydrogen bond analysis for each window (1 ns in duration) on each snapshot (after 1 ps) for G5-PAMAM–ligand complex. Each window is shown with a different color for easy comparison. On the x axis, different numbers represent a single window with their assumed equilibrium distances in Å (not to be confused as distance along the axis).

to be approximately 9 kcal/mol, as compared to G5-PAMAM–Pbz for which it was calculated to be 42 kcal/mol. From these PMF values, we can draw two important conclusions: (i) the encapsulation and subsequent release of a Pbz drug molecule can occur easily because of a low energy barrier in the case of G5NP-PAMAM ($\text{pH} \approx 10$), and (ii) when the pH is lowered (to $\text{pH} \approx 7$), the free energy barrier will be high, and hence, the encapsulated Pbz drug molecule bound to G5-PAMAM will be released with difficulty compared to G5NP-PAMAM.

There are some studies in the literature that account for the difficulty in encapsulation of hydrophobic drugs into the host dendrimer at lower pH values. In one of the studies, Devarakonda et al.⁵⁶ found the nonpolar cavities present inside the dendrimer core to be useful to encapsulate the hydrophobic

drugs by hydrophobic interactions, but at lower pH values, they observe these nonpolar cavities present inside the dendrimer core to change into a more polar one. This has happened because of the protonation of tertiary amines in the interior of the dendrimer. As a result, they found difficulty in the encapsulation of hydrophobic drugs into the dendrimer core. In another study, Dufes et al.¹⁰ showed that, at lower pH values of dendrimer solution, the weakly acidic Pbz molecule undergoes ionization poorly and thus exhibits a very weak electrostatic interaction with the cationic dendrimer. All these factors at low pH make it difficult in encapsulating the Pbz drug molecule into the host dendrimer. So, encapsulation of the Pbz drug molecule is facilitated at high pH.

In the case of G5-PAMAM–Pbz, the dendrimer is in protonated form (cationic), and the pH of the dendrimer solution is suitable for the complete ionization of weakly acidic Pbz drug molecule. Thus, the completely ionised Pbz drug molecules exhibit strong electrostatic attraction with the host dendrimer. That is why we observe higher energy barrier for G5-PAMAM–Pbz than G5NP-PAMAM–Pbz.

In another study, Yang et al.⁵⁷ evaluated the binding of Pbz and PAMAM dendrimers by a combination of solubility measurement, 2D-NOESY NMR and isothermal titration calorimetry (ITC) experiments. They observed that PAMAM dendrimers enhance the aqueous solubility of Pbz, and this was in turn found to depend on the dendrimer concentration, generation, surface function group, and pH value, and also, their thermodynamic data from ITC analysis proved the presence of strong electrostatic interactions between the positively charged dendrimers (at pH 7) and the Pbz molecule. We find a similar strong electrostatic interaction between the G5-PAMAM dendrimer and Pbz drug molecule in our study.

In another related study, Pistolis et al.⁵⁸ demonstrated the pH dependent expulsion of pyrene from the interior of poly(propyleneimine) dendrimers. They observed encapsulation of a pyrene ligand to occur at an easier rate when the pH is higher. At lower pH, they found protonation of internal dendrimer amines leading to polar environment and thus resulting in expulsion of pyrene from the core of the poly(propyleneimine) dendrimer.

In order to substantiate our results further, we have performed PMF study on the G5NP-PAMAM dendrimer complexed with Sal (one of the soluble ligand). In this case, also, we observe the free energy barrier to be very low for G5NP-PAMAM–Sal (~3 kcal/mol) compared to the protonated G5-PAMAM–Sal complex for which it was calculated to be 14 kcal/mol (see Figure 3). We have also computed the different contributions to the total energy of the PAMAM–guest molecule systems using the MM-PBSA/GBSA^{59,60} tool in AMBER 9 (see Supporting Information). Electrostatic contribution dominates compared to van der Waals interaction. We see that for the nonprotonated G5 case, the electrostatic interaction for drugs like Sal is very low and thus making the free energy barriers for G5NP–Sal very low.

From these results, we suggest that the encapsulation of a drug molecule into the host PAMAM dendrimer should be carried out at higher pH values (near pH 10), and at near neutral pH (7.4), we can see strong binding between the drug molecule and the host dendrimer. So, when the dendrimer–drug complex enters the human body, the pH is around 7.4, and thus, the dendrimer holds the drug tightly. Hence, the release of drug occurs at a controlled rate into the bloodstream.

4. SUMMARY AND CONCLUSIONS

In this work, we have carried out atomistic MD simulation to study the interaction behavior between the PAMAM dendrimer of G5 and the four ligands (Sal, Ala, Prim, and Pbz). We analyzed the release pattern behavior of four ligands that were encapsulated inside the dendrimer by measuring the potential of mean force. We see the order of ease of release of drugs from the protonated dendrimer to be Ala > Sal > Prim > Pbz. The soluble drugs (Sal and Ala) were found to have a lower free energy barrier than that of the insoluble drugs (Pbz and Prim), and also, from the hydrogen bond analysis, we see that the intermolecular hydrogen bonding does not contribute much in raising the free energy barrier. We also observe relatively low

energy free barrier: ~9 and 3 kcal/mol for G5NP-PAMAM–Pbz and G5NP-PAMAM–Sal systems, respectively. From our results, we learn that PMF is lower when the same drug is bound to nonprotonated dendrimer instead of protonated dendrimer. These findings suggest that drugs to be entrapped into the host (dendrimer) at higher pH (around 10), which causes lesser PMF barrier or, in other sense, ease in entrapment of molecules inside the dendrimer. So, in the host dendrimer, drug encapsulation should be carried out at higher pH values. Our present study thus provides significant insight about the encapsulation and the release pattern of drugs in the case of dendrimer-based host–guest systems.

■ ASSOCIATED CONTENT

Supporting Information

Various GAFF atom types along with the RESP charges for all the four drugs (Ala, Sal, Prim, and Pbz), energy contribution analysis of G5–Sal and G5NP–Sal, and radius of gyration plot for all the cases. This material is available free of charge via the Internet at <http://pubs.acs.org>.

■ AUTHOR INFORMATION

Corresponding Author

*E-mail: maiti@physics.iisc.ernet.in.

Notes

The authors declare no competing financial interest.

■ ACKNOWLEDGMENTS

We thank DBT, India, for financial support.

■ REFERENCES

- (1) Cai, X. J.; Xu, Y. Y. *Cytotechnology* **2011**, 63, 319–323.
- (2) Singh, R.; Nalwa, H. S. *J. Biomed. Nanotechnol.* **2011**, 7, 489–503.
- (3) Zhou, H.; Lee, J. *Acta Biomater.* **2011**, 7, 2769–2781.
- (4) Wang, M.; Thanou, M. *Pharmacol. Res.* **2010**, 62, 90–99.
- (5) Boas, U.; Heegaard, P. M. H. *Chem. Soc. Rev.* **2004**, 33, 43–63.
- (6) Esfand, R.; Tomalia, D. A. *Drug Discovery Today* **2001**, 6, 427–436.
- (7) Tekade, R. K.; Kumar, P. V.; Jain, N. K. *Chem. Rev.* **2008**, 109, 49–87.
- (8) Gupta, U.; Agashe, H. B.; Asthana, A.; Jain, N. K. *Biomacromolecules* **2006**, 7, 649–658.
- (9) D'Emanuele, A.; Attwood, D. *Adv. Drug Delivery Rev.* **2005**, 57, 2147–2162.
- (10) Dufès, C.; Uchegbu, I. F.; Schätzlein, A. G. *Adv. Drug Delivery Rev.* **2005**, 57, 2177–2202.
- (11) Longmire, M.; Choyke, P. L.; Kobayashi, H. *Curr. Top. Med. Chem.* **2008**, 8, 1180–1186.
- (12) Vasumathi, V.; Maiti, P. K. *Macromolecules* **2010**, 43, 8264–8274.
- (13) Krishna, T. R.; Jayaraman, N. *Tetrahedron* **2004**, 60, 10325–10334.
- (14) Reek, J. N. H.; Arévalo, S.; van Heerbeek, R.; Kamer, P. C. J.; van Leeuwen, P. W. N. M.; Bruce, C. G. A. H. K. *Dendrimers in Catalysis*. In *Advances in Catalysis*; Academic Press: New York, 2006; Vol. 49, pp 71–151.
- (15) Twyman, L. J.; King, A. S. H.; Martin, I. K. *Chem. Soc. Rev.* **2002**, 31, 69–82.
- (16) Caminade, A. M.; Servin, P.; Laurent, R.; Majoral, J. P. *Chem. Soc. Rev.* **2008**, 37, 56–67.
- (17) Adronov, A.; Frechet, J. M. J. *Chem. Commun.* **2000**, 1701–1710.
- (18) Bhadra, D.; Bhadra, S.; Jain, N. K. *Pharm. Res.* **2006**, 23, 623–633.

- (19) Bhadra, D.; Bhadra, S.; Jain, N. K. *J. Pharm. Pharm. Sci.* **2005**, *8*, 467–482.
- (20) Bhadra, D.; Bhadra, S.; Jain, N. K. *J. Drug. Delivery Sci. Technol.* **2005**, *15*, 65–73.
- (21) Bhadra, D.; Bhadra, S.; Jain, S.; Jain, N. K. *Int. J. Pharm.* **2003**, *257*, 111–124.
- (22) Gajbhiye, V.; Kumar, P. V.; Tekade, R. K.; Jain, N. K. *Curr. Pharm. Des.* **2007**, *13*, 415–429.
- (23) Menjoge, A. R.; Kannan, R. M.; Tomalia, D. A. *Drug Discovery Today* **2010**, *15*, 171–185.
- (24) Astruc, D.; Boisselier, E.; Ornelas, C. *Chem. Rev.* **2010**, *110*, 1857–1959.
- (25) Fernandez, L.; Gonzalez, M.; Cerecetto, H.; Santo, M.; Silber, J. *J. Supramol. Chem.* **2006**, *18*, 633–643.
- (26) Klajnert, B.; Stanislawski, L.; Bryszewska, M.; Palecz, B. *Biochim. Biophys. Acta, Proteins Proteomics* **2003**, *1648*, 115–126.
- (27) Hu, J.; Cheng, Y.; Wu, Q.; Zhao, L.; Xu, T. *J. Phys. Chem. B* **2009**, *113*, 10650–10659.
- (28) Cheng, Y.; Wu, Q.; Li, Y.; Xu, T. *J. Phys. Chem. B* **2008**, *112*, 8884–8890.
- (29) Jansen, J. F. G. A.; de Brabander-van den Berg, E. M. M.; Meijer, E. W. *Science* **1994**, *266*, 1226–1229.
- (30) Hu, J.; Cheng, Y.; Ma, Y.; Wu, Q.; Xu, T. *J. Phys. Chem. B* **2008**, *113*, 64–74.
- (31) Boisselier, E.; Ornelas, C.; Pianet, I.; Aranzaes, J. R.; Astruc, D. *Chem.—Eur. J.* **2008**, *14*, 5577–5587.
- (32) Zhao, L.; Cheng, Y.; Hu, J.; Wu, Q.; Xu, T. *J. Phys. Chem. B* **2009**, *113*, 14172–14179.
- (33) Santo, M.; Fox, M. A. *J. Phys. Org. Chem.* **1999**, *12*, 293–307.
- (34) Zhao, L.; Wu, Q.; Cheng, Y.; Zhang, J.; Wu, J.; Xu, T. *J. Am. Chem. Soc.* **2010**, *132*, 13182–13184.
- (35) Miklis, P.; Cagin, T.; Goddard, W. A. *J. Am. Chem. Soc.* **1997**, *119*, 7458–7462.
- (36) Teobaldi, G.; Zerbetto, F. *J. Am. Chem. Soc.* **2003**, *125*, 7388–7393.
- (37) Ivanov, A. A.; Jacobson, K. A. *Bioorg. Med. Chem. Lett.* **2008**, *18*, 4312–4315.
- (38) Chasse, T. L.; Sachdeva, R.; Li, Q.; Li, Z.; Petrie, R. J.; Gorman, C. B. *J. Am. Chem. Soc.* **2003**, *125*, 8250–8254.
- (39) Quintana, A.; Raczka, E.; Piehler, L.; Lee, I.; Myc, A.; Majoros, I.; Patri, A.; Thomas, T.; Mulé, J.; Baker, J. *Pharm. Res.* **2002**, *19*, 1310–1316.
- (40) Teobaldi, G.; Zerbetto, F. *J. Lumin.* **2005**, *111*, 335–342.
- (41) Lee, I.; Athey, B. D.; Wetzel, A. W.; Baker, J. R. J. Molecular Dynamics Studies on Folic Acid and Fluorescein-Derivatized PAMAM Dendrimers; Technical Proceedings of the 2001 International Conference on Computational Nanoscience and Nanotechnology, South Carolina, 2001.
- (42) Tanis, I.; Karatasos, K. *J. Phys. Chem. B* **2009**, *113*, 10984–10993.
- (43) Evangelista-Lara, A.; Guadarrama, P. *Int. J. Quantum Chem.* **2005**, *103*, 460–470.
- (44) Zhang, Y.; Thomas, T. P.; Lee, K.-H.; Li, M.; Zong, H.; Desai, A. M.; Kotlyar, A.; Huang, B.; Banaszak Holl, M. M.; Baker, J. R. Jr. *Bioorg. Med. Chem.* **2011**, *19*, 2557–2564.
- (45) Torrie, G. M.; Valleau, J. P. *J. Comput. Phys.* **1977**, *23*, 187–199.
- (46) Maingi, V.; Jain, V.; Bharatam, P. V.; Maiti, P. K. Submitted for publication, 2011.
- (47) Frisch, M. J.; Trucks, G. W.; Schlegel, H. B.; Scuseria, G. E.; Robb, M. A.; Cheeseman, J. R.; Montgomery, J. A., Jr.; Vreven, T.; Kudin, K. N.; Burant, J. C.; Millam, J. M.; Iyengar, S. S.; Tomasi, J.; Barone, V.; Mennucci, B.; Cossi, M.; Scalmani, G.; Rega, N.; Petersson, G. A.; Nakatsuji, H.; Hada, M.; Ehara, M.; Toyota, K.; Fukuda, R.; Hasegawa, J.; Ishida, M.; Nakajima, T.; Honda, Y.; Kitao, O.; Nakai, H.; Klene, M.; Li, X.; Knox, J. E.; Hratchian, H. P.; Cross, J. B.; Bakken, V.; Adamo, C.; Jaramillo, J.; Gomperts, R.; Stratmann, R. E.; Yazyev, O.; Austin, A. J.; Cammi, R.; Pomelli, C.; Ochterski, J. W.; Ayala, P. Y.; Morokuma, K.; Voth, G. A.; Salvador, P.; Dannenberg, J. J.; Zakrzewski, V. G.; Dapprich, S.; Daniels, A. D.; Strain, M. C.; Farkas, O.; Malick, D. K.; Rabuck, A. D.; Raghavachari, K.; Foresman, J. B.; Ortiz, J. V.; Cui, Q.; Baboul, A. G.; Clifford, S.; Cioslowski, J.; Stefanov, B. B.; Liu, G.; Liashenko, A.; Piskorz, P.; Komaromi, I.; Martin, R. L.; Fox, D. J.; Keith, T.; Al-Laham, M. A.; Peng, C. Y.; Nanayakkara, A.; Challacombe, M.; Gill, P. M. W.; Johnson, B.; Chen, W.; Wong, M. W.; Gonzalez, C.; Pople, J. A. *Gaussian 03*, revision C.02; Gaussian, Inc.: Wallingford, CT, 2003.
- (48) Case, D. A.; Darden, T. A.; Cheatham III, T. E.; Simmerling, C. L.; Wang, J.; Duke, R. E.; Luo, R.; Merz, K. M.; Pearlman, D. A.; Crowley, M. *AMBER 9*; University of California: San Francisco, CA, 2006.
- (49) Wang, J.; Wolf, R. M.; Caldwell, J. W.; Kollman, P. A.; Case, D. A. *J. Comput. Chem.* **2004**, *25*, 1157–1174.
- (50) Trott, O.; Olson, A. J. *J. Comput. Chem.* **2010**, *31*, 455–461.
- (51) Morris, G. M.; Goodsell, D. S.; Halliday, R. S.; Huey, R.; Hart, W. E.; Belew, R. K.; Olson, A. J. *J. Comput. Chem.* **1998**, *19*, 1639–1662.
- (52) Jorgensen, W.; Chandrasekhar, J.; Madura, J.; Impey, R.; Klein, M. *J. Chem. Phys.* **1983**, *79*, 926–935.
- (53) Ryckaert, J.-P.; Ciccotti, G.; Berendsen, H. J. C. *J. Comput. Phys.* **1977**, *23*, 327–341.
- (54) Berendsen, H.; Darden, T.; York, D.; Pedersen, L. *J. Chem. Phys.* **1993**, *98*, 10089–11092.
- (55) Grossfield, A. WHAM: an implementation of the weighted histogram analysis method. <http://membrane.urmc.rochester.edu/content/wham>, version 2.0.4.
- (56) Devarakonda, B.; Hill, R. A.; de Villiers, M. M. *Int. J. Pharm.* **2004**, *284*, 133–140.
- (57) Yang, W.; Li, Y.; Cheng, Y.; Wu, Q.; Wen, L.; Xu, T. *J. Pharm. Sci.* **2009**, *98*, 1075–1085.
- (58) Pistolis, G.; Malliaris, A.; Tsiourvas, D.; Paleos, C. M. *Chem.—Eur. J.* **1999**, *5*, 1440–1444.
- (59) Gohlke, H.; Case, D. A. *J. Comput. Chem.* **2004**, *25*, 238–250.
- (60) Kollman, P. A.; Massova, I.; Reyes, C.; Kuhn, B.; Huo, S.; Chong, L.; Lee, M.; Lee, T.; Duan, Y.; Wang, W.; Donini, O.; Cieplak, P.; Srinivasan, J.; Case, D. A.; Cheatham, T. E. *Acc. Chem. Res.* **2000**, *33*, 889–897.